Physicochemical properties of tire-derived *para*-phenylenediamine quinones - A comparison of experimental and computational approaches

Simon H. Maguire,[a] Misha Zvekic, [a,b] Angelina Jaeger,[a,b] Joseph Monaghan,[a,b] Erik T. Krogh,[a,b] and Heather A. Wiebe [a,b]

[a] Department of Chemistry, Vancouver Island University, 900 Fifth Street, Nanaimo BC
[b] Department of Chemistry, University of Victoria, 3800 Finnerty Rd, Victoria, BC

Para-phenylenediamine (PPD) compounds are added to tire rubber at percent levels to sacrificially react with oxidants for prolonged service life. Recently, the PPD transformation product *N*-(1,3-dimethylbutyl)-*N*'-phenyl-*p*-phenylenediamine quinone (6PPDQ) has been identified in roadway runoff as a potent toxicant for coho salmon (*Oncorhynchus kisutch*). As 6PPD may be phased out in favour of alternative PPDs, understanding the physicochemical properties of their corresponding quinones is important for predicting their environmental fate, distribution, and toxicity. Here, we present experimentally determined water solubility values for 6PPDQ and five structural analogues and find them to be several orders of magnitude lower than those predicted by EPI Suite, a popular Quantitative Structure Activity Relationship (QSAR) program. We also report octanol-water and air-water partition coefficients for PPDQs using Density Functional Theory (DFT) and QSAR approaches. Both methods provided similar rank ordering of compounds. However, DFT methods tended to underestimate log K_{ow} values and overestimate log K_{aw} values relative to EPI Suite. We discuss the strengths and limitations of both computational approaches, the need for more experimentally derived values, and caution researchers interpreting predicted physicochemical properties, particularly for emerging contaminants for which QSARs may be poorly parameterized.

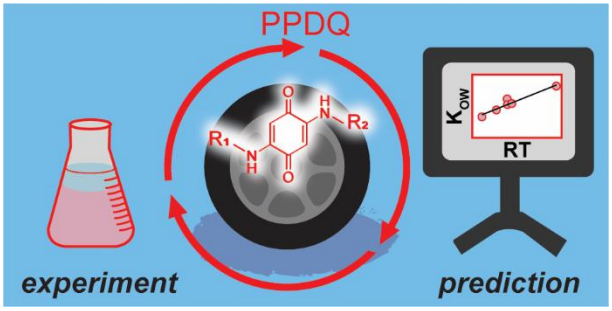

Keywords: tire wear toxins, solubility, partition coefficients, EPI Suite, Density Functional Theory, para-phenylenediamine quinones, Quantitative Structure Activity Relationships

Environmental Significance statement (120 words):

Tire wear particles have been identified as a source of *N*-(1,3-dimethylbutyl)-*N*'-phenyl-*p*-phenylenediamine quinone (6PPDQ), which leads to Urban Runoff Mortality Syndrome in salmonid species. Characterizing the physicochemical properties of 6PPDQ and structurally related *para*-phenylenediamine quinone analogues (PPDQs) is crucial in understanding their environmental fate, distribution, and consequent risks towards aquatic organisms. Computational methods can provide important insight into intrinsic molecular properties, especially where compounds are unavailable in sufficient quantity and/or purity to carry out experimental measurements. This paper presents experimental water solubilities and evaluates several computational methods applied to PPDQs of

emerging concern. The research is significant in the evaluation of alternative tire preservatives as well as fate and distribution models that inform the design of engineered treatment systems.

Introduction

In 2021, Tian *et al.* identified *N*-(1,3-dimethylbutyl)-*N*'-phenyl-*p*-phenylenediamine quinone (6PPDQ) as the cause of rain driven mass die-off events of coho salmon (*Oncorhynchus kisutch*) in the Pacific Northwest – a phenomenon known as Urban Runoff Mortality Syndrome (URMS).[1] *Para*-phenylenediamine quinones (PPDQs) are derived from the ozonation of *para*-phenylenediamines (PPDs), sacrificial antiozonants added at 0.4–2 wt% to tire rubber to extend their use.[1] 6PPDQ and structurally related PPDQ analogues have been observed to enter urban waterways and have been quantified in road dust, sediments, snowmelt, fish tissues, and other matrices.[2–8] 6PPDQ toxicity has been established for other salmonid species, including brook trout (*Salvelinus fontinalis*),[9–11] rainbow trout (*Oncorhynchus mykiss*),[9,10] and lake trout (*Salvelinus namaycush*),[12] but coho salmon appear to be the most susceptible with LC_{50} values ranging from 41–95 ng/L.[13,14] 6PPDQ appears to exhibit stereoselective toxicity, as the S enantiomer was recently reported to be 2.6 times more toxic to coho salmon than the R enantiomer.[9,15] The 2024 U.S. Tire Manufacturers Association Preliminary (Stage 1) Alternatives Analysis Report proposes several alternatives to 6PPD,[16] including structural analogs where alkyl/aryl groups (R_1 and R_2) are varied (Figure 1 and Figure S1). However, the physicochemical properties of 6PPDQ and related analogs remain largely unreported.

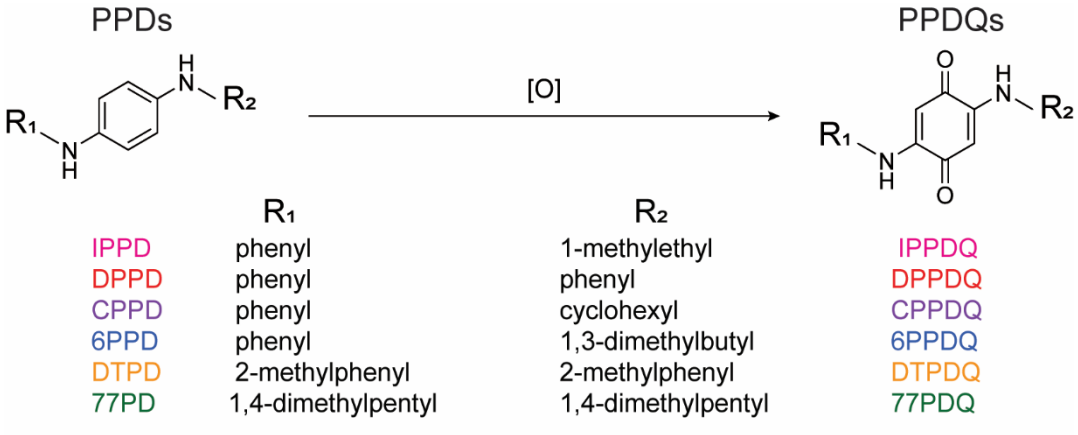

Figure 1. Structurally related PPD and PPDQ compounds discussed in this work.

The physicochemical properties of a contaminant govern its environmental fate and distribution behaviour, including physical, chemical, and biological processes.[17] Characterization of these intrinsic properties enables more accurate multi-phase models thus improving our understanding of the impact of environmental contaminants.[18] Knowledge of these properties also informs appropriate sample handling in both the field and the lab. For example, recent studies have demonstrated that 6PPDQ sorbs to hydrophobic plastic laboratory materials and is lost from aqueous samples open to the atmosphere.[4,19,20] Understanding these loss processes is critical in developing good laboratory practices for analytical determinations and has important implications for exposure and toxicity studies.

Of particular interest for PPDQs is their water solubility, a property which gives an upper bound to their ability to leach from tire wear particles into the aquatic environment and contributes to both the air-water (K_{aw}) and octanol-water (K_{ow}) partition coefficients. Compounds with low water solubility such as 6PPDQ[19] pose a challenge when constructing aqueous standards or designing toxicity studies, especially if the solubility limits are exceeded. Various structural and thermodynamic factors influence water solubility including the strength of the solvent-solute interactions and the partial molar volume of the compound, both of which affect the energetics of cavity formation in water. Water solubility can be measured in several ways, but generally involves measuring the concentration of the solute in a saturated solution of fixed composition and temperature.[17] Complicating the measurement of aqueous solubility, sparingly soluble hydrophobic compounds can be slow to dissolve into water from their pure solid or liquid form, have a tendency to partition to container walls as well as the air-water interface, and may in some cases self-aggregate into dimers, micelles and other lamellar structures.[21]

Additional challenges in experimentally measuring physicochemical properties of emerging contaminants may arise due to cost (time, personnel, instrumentation), toxicity concerns, and low availability of pure standards. The latter concern is particularly relevant for transformation products such as PPDQs,[19,22] as not all quinone products of proposed PPD alternatives are commercially available and

those that are may be prohibitively expensive. In such circumstances, physicochemical properties may be predicted using a variety of computational tools. A common approach is Quantitative Structure Activity Relationship (QSAR) models, such as EPI Suite.[23] QSAR modelling involves comparing structural moieties of the target compound to a training set of compounds with well-characterized physicochemical properties to generate predicted properties. As such, the predictive model is most accurate when the target compound is structurally similar to the training set, which can limit the accuracy of predictions for complex molecules or unusual structural moieties like those found in PPDQs. EPI Suite in particular uses two dimensional SMILES codes as input, so cannot account for variation introduced by chiral centres, protonation states, or pH effects.[24,25] Predicted properties of PPDQs have previously been reported by Klockner *et al.* (2021), Cao *et al.* (2022), and Zeng *et al.* (2023) using QSARs methods,[26–28] however the accuracy of these values has not been evaluated. Given the structural complexity of PPDQs and the relative novelty of the electron distribution in phenylenediamine quinones, it is unclear if the available training data in EPI Suite and other QSAR models yield accurate predictions for PPDQs. This led us to consider density functional theory (DFT) as an alternative computational approach to evaluate PPDQs. Unlike QSAR models, DFT methods are not based on experimentally derived properties. Instead, they use quantum mechanics to calculate the electronic structure of a molecule from first principles, which is then used to compute the desired property.[29,30] As DFT does not rely on empirical data, properties calculated using this method may be more accurate for molecules with novel moieties that are not well parameterized.[31] However, relative to QSAR approaches, DFT calculations are computationally expensive and can require several days of run time on a supercomputer. Simplifying assumptions about the system such as the use of a dielectric continuum to represent the solvent rather than the use of discrete solvent molecules can reduce the run time.[32,33] Regardless of the computational approach, experimentally-derived results are needed to validate the accuracy of predicated properties and inform simplifying assumptions.

Hu *et al.* recently reported the log K_{ow} and water solubility of 6PPDQ to be 4.30 ± 0.02 and 38 ± 10 µg L^{-1}, respectively.[19] Interestingly, EPI Suite predicts a similar log K_{ow} (3.98) but a water solubility value over three orders of magnitude greater at 56.9 mg L^{-1}.[27] This discrepancy, along with the general lack of physicochemical property information available for the PPDQ structural analogs, prompted us to examine this further. Here, we compare water solubility predictions made by EPI Suite for six PPDQs to experimental values made by directly measuring their free concentration in aqueous solution using condensed phase membrane induction mass spectrometry (CP-MIMS).[34] Additionally, we evaluate the suitability of DFT methods relative to QSARs for the calculation of the environmentally relevant partition coefficients K_{ow} and K_{aw}.

Experimental Materials and Methods

Experimental Materials

Deionized water (18 MΩ-cm, Facility Scale Reverse Osmosis/Ion Exchange Water Purification System, Applied Membranes Inc., Vista, CA, USA) was used to prepare analytical standards. HPLC-grade solvents were purchased from Fisher Scientific (Ottawa, ON). 6PPDQ, 6PPDQ-d_5, IPPDQ, 77PDQ, DTPDQ, DPPDQ, and CPPDQ were obtained from HPC Standards Inc (>92% purity, Atlanta, GA, USA). $^{13}C_6$-6PPDQ was purchased from ACP Chemicals (Montreal, QC, CAN).

Water Solubility

The aqueous phase concentrations of PPDQs were monitored in real-time using a semi-permeable membrane immersion probe mounted into a Teflon-backed cap screwed onto the sample vial. This approach, termed condensed phase membrane introduction mass spectrometry (CP-MIMS), has been described previously.[4] Here, the probe consisted of an 8.0 cm long, 170 µm thick (0.30 mm ID, 0.64 mm OD) hollow fibre polydimethylsiloxane (PDMS) membrane (Silastic brand, Dow Corning, Midland, MI, USA)

mounted onto 22-gauge stainless-steel hypodermic tubing. The acceptor phase was a 15/85 (*v/v)* heptane/methanol solution containing 20 µg kg^{-1} $^{13}C_6$-6PPDQ internal standard (IS) acidified with 0.03% formic acid (Fisher Chemical, Ottawa, ON). Acceptor phase was continuously delivered at 10 µL min^{-1} *via* syringe pump (Chemyx Fusion 100, Stafford, TX, USA) with a 10 mL gas-tight syringe (Hamilton 1000 series, Fisher Scientific) to an electrospray ionization (ESI) source. Analysis was conducted using positive mode ESI coupled to a triple quadrupole mass spectrometer (ESI-MS/MS; Perkin-Elmer QSight™ 220, Waltham, MA, USA). Instrument parameters and MS/MS transitions are listed in Table S1. Water solubility was determined by monitoring changes in the IS-normalized MS/MS signal intensity in response to sequential spike additions of an analytical standard solution of individual PPDQs. Each spike addition was followed by a 10-minute stabilization period in a continuously-stirred, temperature-controlled solution at 25 ± 1 °C for all six PPDQs, with additional experiments at 11 ± 1 and 41 ± 1 °C for 6PPDQ. The internal standard corrected signal intensity is plotted over time (Figure 2) and the solubility was determined using the intersection of the best-fit lines derived from the linear dynamic calibration range and data points in a saturated solution. Solubility experiments were performed in triplicate for 6PPDQ with 13–16 spike additions of 30. µL of 6.9 mg L^{-1} 6PPDQ sub-stock (in acetonitrile) into 37.0 mL of DI water (pH ~ 5.5). This resulted in a final co-solvent concentration of 0.1% *v/v*. A control experiment evaluating the solubility of 6PPDQ at elevated co-solvent concentration (2% *v/v*) showed no significant change to the observed solubility (Figure S2). Temperatures were controlled with a recirculating chiller (2095 Bath and Circulator, Forma Scientific, Marietta, OH, USA) to remain at 25.4 ± 0.2 °C. A sample vial was placed inside a double-walled beaker, and water from the chiller was circulated through the outer layer. The water temperature inside the beaker, equilibrated with the sample, was measured with a digital thermometer. The solubility of the PPDQ analogues were examined using 10. µL spikes of stock solution (in methanol: 1.77 mg L^{-1} DTPDQ, 54.4 mg L^{-1} IPPDQ, 22.1 mg L^{-1} CPPDQ, 2.88 mg L^{-1} 77PDQ, and acetonitrile: 39.4 mg L^{-1} DPPDQ).

Uncertainties were determined from the standard deviation of n = 3 experimental replicates for 6PPDQ and from six different line fits for a single experiment the remaining PPDQs, as illustrated in Figure S3.

Liquid Chromatography and Log K_{ow}

Aqueous solubility for 6PPD, 6PPDQ, and DTPDQ were also analyzed using a more conventional analytical workflow involving liquid chromatography-mass spectrometry of filtered, aqueous solutions. A series of solutions were prepared by spiking increasing volumes of a methanolic standard (280 mg L^{-1} 6PPD, 4.7 mg L^{-1} 6PPDQ, 4.9 mg L^{-1} DTPDQ) into 40 mL vials containing deionized water with 300 ng L^{-1} 6PPDQ-d_5 acting as an internal standard (maximum methanol co-solvent *ca.* 2% *v/v*). Aqueous solutions were equilibrated at room temperature for 10 minutes before filtration through a 0.45 µm Acrodisc Nylon filter (Pall Corporation, Port Washington, NY, USA) *via* a 50 mL glass syringe. Heptane (1.0 mL) was added to the aqueous filtrate, and the solution was then shaken for 30 seconds and allowed to fully separate. A 500. µL aliquot of the heptane layer was taken for HPLC-MS analysis with a Thermo Fisher Vanquish MD HPLC connected to a TSQ Fortis. A YMC Triart C18 column (100 x 2.1 mm, 3 µm; Chromatographic Specialties, Brockville, ON, CAN) was used at 35 °C. Sample injections were 2.00 µL into an isocratic 0.200 mL min^{-1} flow of 0.1% *v/v* formic acid in methanol. The same *m/z* transitions described above (Table S1) were employed, with additional mass spectrometer settings listed in the table footnote. Chromatographic peak areas normalized to the internal standard were plotted against the added concentration.

The K_{ow} for 6PPDQ was determined following the method of Hu *et al.* with minor modifications, including 30 minutes of equilibration in an ultrasonic bath and separation *via* centrifugation at 2500 RPM for 60 minutes.[19] Quantitation of 6PPDQ in the aqueous and *n*-octanol phase was determined by HPLC–MS/MS using solvent matched calibration standards ranging from 0.5−12 µg L^{-1} and 0.6−48 µg L^{-1}, respectively. To aid in the discussion of computational K_{ow} values for the structurally related PPDQ series, we obtained isocratic retention times with 25/75 (*v/v*) water/methanol eluent with 0.1% (*v/v*) formic acid (Figure S4, Table S2).

Computational Methods - EPI Suite

The Estimation Program Interface (EPI) Suite (v4.11) provided by the US EPA predicts physicochemical properties using the two-dimensional SMILES code of a compound and quantitative structure activity relationships (QSARs).[23] Programs within EPI Suite use either a bond contribution or a group contribution method, wherein a molecule is divided into a set of covalent bonds or groups of atoms, each of which have been parameterized with a contribution towards a given physicochemical property based on experimental data. The predicted property is therefore the sum of the contributions from each bond or group, plus correction factors. The KOWWIN Program (v1.68) was used to predict log K_{ow} values with the group contribution method. The bond contribution method in the HENRYWIN Program (v3.20) predicted Henry's law constants at 25°C in $Pa \cdot m^3\ mol^{-1}$ which were converted to K_{aw} values *via* the ideal gas law (Eqn. S1). The HENRYWIN group contribution method did not output a prediction for the PPDQs as it is missing a value for the secondary amine. Water solubility (C_W^{sat}) was calculated from K_{ow} with WSKOWWIN (v1.42) using equation S2 and from the group contribution method with WATERNT (v1.01).

Computational Methods - Density functional theory

DFT calculations were performed using Gaussian 16 (revision c.01)[35] with the ωB97XD exchange-correlation functional and the 6-311++G(d,p) basis set. Molecular geometries of 6PPD, 6PPDQ and its analogues were optimized, and the Gibbs energy of each molecule was calculated in the gas phase as well as in implicit water and *n*-octanol using the SMD solvation model.[33] Gibbs energies of solvated systems G_{solv} were calculated using Eqn. 1, where G_{gas} is the Gibbs energy obtained in the gas phase, $E_{gas}(el)$ and $E_{solv}(el)$ are the electronic energy calculated in the gas phase and in implicit solvent respectively, and RT ln (24.46) is a correction factor that accounts a change of reference state from $p^{\ominus}$ = 1 bar in the gas phase to $c^{\ominus}$ = 1 M in solution.

$$G_{solv} = \left[G_{gas} - E_{gas}(el)\right] + E_{solv}(el) + RT \ln 24.46 \quad \text{(Equation 1)}$$

For K_{aw} calculations, G_{gas} was taken directly from Gaussian output with no additional calculation necessary. The K_{ow} and K_{aw} were calculated using Eqn. 2 where ΔG is the Gibbs energy difference for the transition from water to either *n*-octanol or gas phase, *R* is the gas constant, and *T* is 298 K.

$$K = e^{-\frac{\Delta G}{RT}} \qquad \text{(Equation 2)}$$

Estimation of Partial Molar Volumes

Partial molar volumes of PPDQs were calculated using the Archimedean Displacement Model,[38,39] a molecular-dynamics based method for accurate determinations of molecular volumes. In this technique, classical force fields are used to represent intra- and inter-molecular interactions, which allows for explicit solvent molecules to be included in the calculation. The partial molar volume of a solute surrounded by N explicit solvent molecules is determined by the amount of displaced volume relative to the pure N-solvent system when a single molecule of solute is added. Simulations were performed using GROMACS 2023 and the OPLS/AA force field,[38-41] in a cubic periodic box containing about 2000 solvent molecules and one solute. Temperature was maintained at 298 K with the velocity-rescale thermostat (τ_T = 0.1 ps)[36] and pressure was maintained at 1 bar with the C-rescale barostat (τ_P = 2.0 ps).[37]

Results & Discussion

Water solubility

To determine the water solubility of 6PPDQ and its analogs, we employed a semi-permeable membrane immersion probe to directly measure the free aqueous phase concentration *in situ*. This approach was demonstrated previously by Termopoli *et al.,*[38] showing excellent agreement between experimental and literature values for the water solubility of pyrene at 135 µg L^{-1}. Figure 2A shows an example chronogram representing the internal standard-normalized MS/MS signal for 6PPDQ over time as consecutive spike additions were added to the aqueous solution. Figure 2B displays the resulting data wherein the signal is plotted against the added concentration. The intersection of the linear portion of the

calibration curve (below the solubility limit, black data points) and the data points clearly above the solubility limit (red data points) corresponds to the solubility limit. Using this approach, we determined the water solubility of 6PPDQ at 25 °C as 31 ± 5 µg L^{-1} which is in excellent agreement with the reported literature value (38 ± 10 µg L^{-1}).[19] We observed that the solubility of 6PPDQ was relatively invariant with temperature ranging from 29 ± 4 (n=3) to 42 ± 6 (n=3) µg L^{-1} between 11 and 41 °C (example plots given in Figure S5).

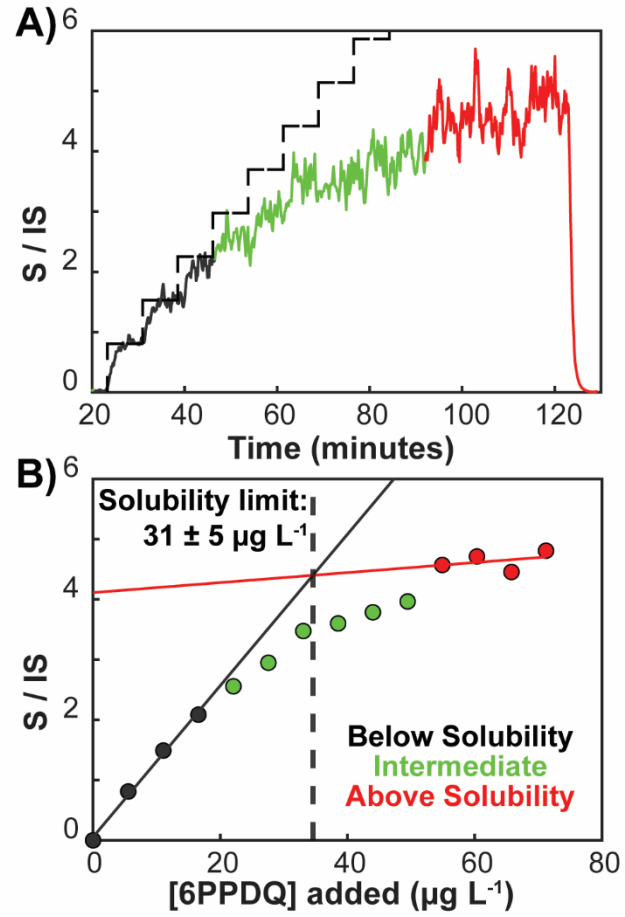

Figure 2. Representative solubility experiment for 6PPDQ. A) The chronogram of the internal standard-normalized MS/MS signal changing over time as spike additions of 6PPDQ are added to aqueous solution (stepwise added concentration change indicated with a dashed line), and B) the resulting normalized signal response at concentrations below (black data), above (red data), and at intermediate (green data) added concentration.

The experimental solubilities of PPDQ analogues are presented in Figure S6 and summarized in Table 1. The water solubility varies across this series with roughly a 50-fold difference between DPPDQ (168 µg L-

[1]) and DTPDQ (3.5 μg L^{-1}). In general, smaller PPDQs, such as IPPDQ and DPPDQ, exhibit higher water solubilities (> 100 μg L^{-1}), whereas the larger DTPDQ and 77PDQ are considerably less water soluble (< 10 μg L^{-1}). 6PPDQ and CPPDQ exhibit intermediate solubilities at 31 and 32 μg L^{-1}, respectively.

Table 1. Comparison of the experimental and calculated water solubility at 25 °C.

Compound	MW (g mol^{-1})	Partial Molar Volume (cm^3 mol^{-1})	CP-MIMS Method (μg L^{-1})	WATERNT (EPI Suite) (μg L^{-1})	WSKOWWIN (EPI Suite) (μg L^{-1})	Corrected WSKOWWIN (μg L^{-1})**
IPPDQ	256.3	207 ± 1	106 ± 6 (410 ± 20 nM)	2.8×10^7	1.4×10^6	850
DPPDQ	290.3	221 ± 1	168 ± 8 (580 ± 30 nM)	6.2×10^4	1.5×10^4	96
CPPDQ	296.4	237 ± 1	32 ± 3 (120 ± 1 nM)	3.1×10^3	5.7×10^4	35
6PPDQ*	298.4	255 ± 2	31 ± 5 (104 ± 15 nM)	1.3×10^6	5.1×10^4	-
DTPDQ	318.4	251 ± 1	3.5 ± 0.3 (11 ± 1 nM)	6.0×10^3	1.2×10^3	7.6
77PDQ	334.5	313 ± 2	6.1 ± 0.8 (18 ± 10 nM)	4.1×10^5	1.7×10^3	1.0

* Literature value for 6PPDQ has been reported to be 38 ± 10 μg L^{-1} following EPA guidelines with minor modifications at 20°C and 67 ± 5 μg L^{-1} at 23°C using a solid/liquid saturator system method.[19,39] Experimental CP-MIMS result for 6PPDQ is reported as the mean and standard deviation of n=3 experiments. All other PPDQ results are based on the mean and standard deviation of three linear fits choosing different points to as below and above solubility for a single experiment. Error on the partial molar volume calculations is estimated using block averaging.[40]

**Recalibrated according to an updated correction term (C=-2.207) in Equation S2 determined from the experimental solubility for 6PPDQ reported here and the EPISuite predicted log K_{ow} available in Table 2.

The observed differences in solubility for the PPDQ analogues are consistent with the expected trend based on their partial molar volumes in water as estimated using the Archimedean Displacement Method (Figure 3).[41–44] The larger an organic contaminant is, the more water-water solvent interactions are disrupted to create a hydrophobic cavity the compound will occupy. This process raises the chemical potential of the solution, consequently reducing the aqueous solubility.[17] As expected for a structurally

related series, a linear free energy relationship was observed between aqueous solubility and estimated partial molar volume, with the exception of DTPDQ which exhibited a low water solubility (3.5 ± 0.3 µg L^{-1}) for its size. Interestingly, the coefficient of determination for the six PPDQs (R^2 = 0.57) improved to 0.90 with the exclusion of DTPDQ (Figure 3). It is worth noting that both DPPDQ and DTPDQ are unique in the PPDQ series as having aryl substituents on both nitrogen atoms, potentially affecting their acid/base characteristics *via* electron delocalization. While beyond the scope of this work, this may lead to consequential pH-dependent solubility for these compounds.

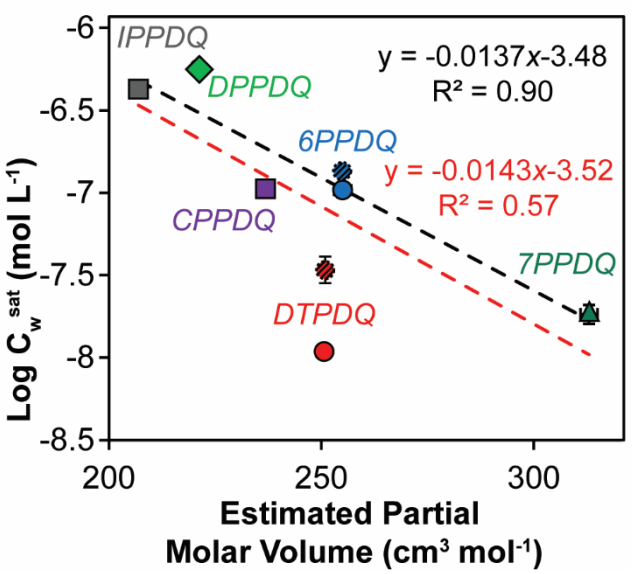

Figure 3. Linear free energy relationship plotting experimental log (C_w^{sat}) from CP-MIMS experiment against calculated partial molar volume using the Archimedean Displacement Method. The red best-fit line includes DTPDQ (R^2 = 0.57) while the black best-fit line excludes it (R^2 = 0.90). Experimental solubilities of 6PPDQ (blue) and DTPDQ (red) determined using an off-line filtration and LC-MS method are illustrated with stripes and are included as a reference (not used in either regression line).

The water solubility of DTPDQ was also measured by preparing a series of aqueous solutions of increasing amounts of DTPDQ, passing them through a 0.45 µm filter, and measuring the resulting concentrations off-line by conventional LC-MS/MS. The solubility of DTPDQ with this approach was determined to be 11 ± 2 µg L^{-1}. While somewhat higher than that measured directly in solution by CP-

MIMS it is still well below the trendline in Figure 3. The solubility of 6PPDQ measured by this method (41 ± 3 µg L^{-1}, Table S3), was in better agreement with the direct CP-MIMS method and also within experimental error of the published value from Hu *et al.*[19] The *in-situ* CP-MIMS data may be revealing solution phase behaviour. In the limit of low concentration, there is a linear dynamic range regime below 10 µg L^{-1} consistent with employing this technique for trace level quantitative 6PPDQ determinations.[4,45] However, at concentrations approaching the saturation limit, the measured free concentration in solution appears to level off gradually (Figure 2; green coloured datapoints). This behaviour suggests some form of self-aggregation at higher concentrations, and appears to be more pronounced for some PPDQs, such as 77PDQ and IPPDQ (Figure S6). Hu *et al.* noted that 6PPDQ can form aggregates based on intermolecular hydrogen bonding and π-π stacking interactions.[19,46] Further computational studies are currently underway to model the energetics of intermolecular interactions of 6PPDQ and structural analogs. In any case, it is worth noting that conventional solubility measurements based on physical separation of dissolved and undissolved phases (i.e., filtration or centrifugation) have the potential to overestimate the solubility of aggregate-forming analytes.

While it remains unclear if all PPDQs are acutely toxic to aquatic organisms, it is clear that they are soluble in water at levels exceeding the LC_{50} of 6PPDQ for coho by several orders of magnitude.[13,14] Additionally, 6PPDQ is considerably less water soluble than the parent compound 6PPD (0.6–2 mg L^{-1}),[39,47] which has likely confounded early toxicity studies reporting experimental designs with concentration levels exceeding the solubility limits reported here.[48] The EPI Suite predicted water solubilities using WSKOWWIN and WATERNT are also included in Table 1. Interestingly, the predicted values are 2–4 orders of magnitude larger than the experimental water solubility reported here and elsewhere.[19,39] Additionally, the predicted water solubilities do not follow the same rank-order trend observed in the experimental results. The accuracy of QSAR methods like WSKOWWIN and WATERNT depend heavily on the similarity of the test molecule to the training set. This training set is publicly available through the most recent

version of the EPI Suite web app (https://episuite.dev/EpiWebSuite/#/) and users are able to view if the database has any structural analogs for a test molecule by using the Analog Identification Methodology (AIM) function. However, there are no analogs for 6PPDQ in the training set at this time. EPI Suite predictions have been found to closely match experimental data for more common compounds like polycyclic aromatic hydrocarbons and monoterpenoids,[49,50] but it is known to deviate from experimental results for more complex structures and novel functional groups.[51–55]

One of the notable characteristics of 6PPDQ is the unusually low basicity of the amine groups, presumably due to the extensive conjugation and electron withdrawing power of the quinone carbonyls. This was first noted in the description of the synthesis of 6PPDQ by Tian *et al.*, where it remained in the organic phase after a wash with 0.1 M HCl to remove more basic impurities.[1] Whereas most organic amines are expected to be protonated under ambient pH conditions and thus more water soluble, this is not the case for 6PPDQ. The EPI Suite QSAR methods may therefore use parameters fitted to reproduce the solubility of compounds with protonated amines, resulting in a significant overestimation of the water solubility of PPDQs. This assertion is supported by the observation that replacing the amines in 6PPDQ with alkane groups in EPI Suite, which would have a similar molar volume but not have parameters that are biased towards protonation, results in a solubility prediction that is 3-4 orders of magnitude closer to the experimental result (130.3 µg/L with WSKOWWIN and 42.9 µg/L with WATERNT). The WSKOWWIN method uses a linear free energy method to predict solubility based on the compound's log K_{ow} and molar mass (Eq. S2) and is therefore more convenient to reparametrize than the fragment-based WATERNT method. We re-fitted the correction term C = 1.008 in Eq. S2 to our experimental solubility and the QSAR predicted log K_{ow} for 6PPDQ (Table 2) and obtained a new value of C' = -2.207, which was used to predict the water solubilities for the remaining analogs. The results, shown in Table 1, are significantly improved over the WSKOWWIN predictions with the original parameters. Therefore, the relatively high hydrophobicity and low basicity of the PPDQs combined with the paucity of experimental data for the

unique enamine quinone structure may explain the poor predictive performance of EPI Suite solubilities for this family of compounds. Therefore, we recommend caution when using this QSAR method for compounds such as PPDQs which are not well-represented by the training set. Additional factors that may give rise to an overestimation of the PPDQ water solubilities by QSAR methods may include water solubility training set data being biased towards compounds with high water solubilities because of historical limitations of analytical measurement sensitivity for hydrophobic organic molecules and/or experimental methods that do not adequately separate molecular clusters from the free aqueous phase compounds.[56] Notably, when the WSKOWWIN method was calculated using Eq. S2 with the original correction term C and the molecular weight of a 6PPDQ dimer, rather than that of a single molecule, the result was closer to experimental findings (6.9×10^2 µg L^{-1} instead of 5.1×10^4 µg L^{-1}, Table 1). We were not able to acquire DFT-based water solubilities due to the lattice energies for these compounds, which is required for such calculations, currently being unknown.

Octanol – Water Partitioning

The octanol-water partition coefficients were calculated using both QSAR (EPI Suite) and DFT (Gaussian) approaches, summarized in Table 2. The predicted K_{ow} values for the PPDQs follow the same rank order by both methods with the KOWWIN values (EPI Suite) being roughly 5 to 10-fold higher. Veith and others[57,58] have employed the correlation between log K_{ow} and log (isocratic retention times) for a structurally related series of compounds to model octanol-water partitioning behaviour. Figure 4 displays this linear free energy relationship for the PPDQ series using our experimental retention times and the predicted log K_{ow} values from DFT and QSAR. The log K_{ow} value of 3.98 predicted by EPI Suite's KOWWIN for 6PPDQ most closely matches our experimental value of 4.0 ± 0.2 as well as that reported earlier by Hu *et al.*[19] of 4.30 ± 0.02 (both overlaid on Figure 4). KOWWIN has been widely accepted to provide good predicted log K_{ow} values for neutral compounds.[59] The calculation of log K_{ow} is one of the most commonly reported uses of EPI Suite in the literature.[52,55,60–62] The DFT method yields a log K_{ow} of 3.27 for 6PPDQ,

which is roughly an order of magnitude less than the experimental values. This discrepancy may be explained by the solvent model used. The implicit SMD solvent model, which uses a dielectric continuum to represent the solvent, has been shown to underestimate log K_{ow} for other compounds.[55,63] The use of dielectric constants for dry *n*-octanol has been shown to yield more accurate results for DFT predictions;[63] however, changing the dielectric here only marginally improved the log K_{ow} result to 3.31. It is important to note that the SMD implicit solvent model does not account for specific solvent-solute interactions such as hydrogen bonding, so inclusion of some explicit solvent molecules around the solute may improve the DFT prediction. However, this would also significantly increase the computational cost of the calculation. Based on the results presented here, we recommend the KOWWIN from EPI Suite for PPDQ analogs.

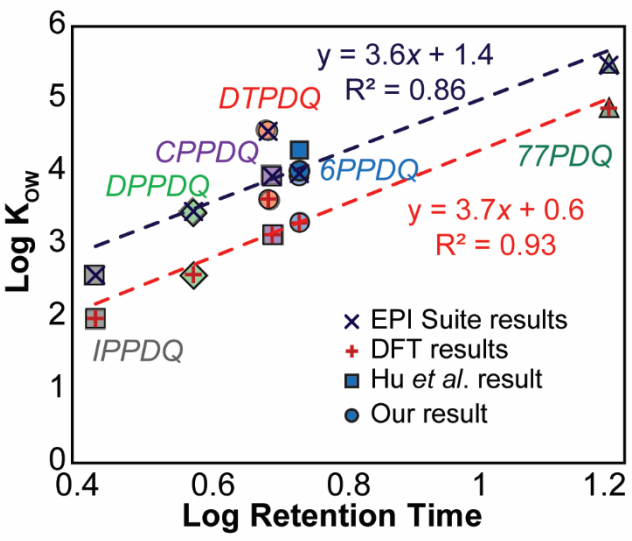

Figure 4. Log-log plot of octanol-water partitioning coefficients against isocratic LC-MS retention times. Calculated log K_{ow} values are denoted with a (+) for DFT calculated values and (x) for QSAR predicted values. Experimental log K_{ow} values for 6PPDQ are superimposed in solid blue for the results reported here (circle) and previously by Hu *et al.* (square).[19]

The predicted log K_{ow} values for the PPDQ analogs examined here range from 2.58 to 5.47, which indicates partitioning into organic matter and biological systems is likely, and is consistent with previous observations of PPDQs in soil/sediment phases.[2,27] While a number of factors such as aquatic toxicity and

environmental persistence need to be considered, the relatively high bioaccumulation potential (log K_{ow} > 3) of many PPDQs poses a significant environmental risk.

Table 2. Calculated log K_{ow} and unitless log K_{aw}

	Log K_{ow}		Log K_{aw}	
Molecule	DFT (Gaussian)	KOWWIN (EPI Suite)	DFT (Gaussian)	HENRYWIN (EPI Suite)
IPPDQ	1.99	2.58	-8.51	-11.71
DPPDQ	2.59	3.46	-8.62	-12.55
CPPDQ	3.14	3.94	-8.65	-11.70
6PPDQ*	3.27	3.98	-7.99	-11.34
DTPDQ	3.63	4.56	-8.92	-12.47
77PDQ	4.84	5.47	-7.18	-9.88
6PPD	4.52	4.68	-5.26	-6.86

*Experimental value for the log K_{ow} of 6PPDQ is 4.0 ± 0.2 in this work and 4.30 ± 0.02 from Hu *et al.* [19]

Air-Water Partitioning

Understanding the air-water partitioning behaviour of PPDQs is important in predicting their environmental distribution and in particular their ability to undergo gas-phase atmospheric transport. A marked decrease in the aqueous concentration of PPDQs when left in open containers exposed to the atmosphere ($t_{1/2}$ ~ 14–108 hrs)[4] has been observed by us and others,[2,4] suggesting that air/water-interface partitioning or some other loss process (e.g., reaction with an atmospheric component) may be occurring. To probe this further, we have calculated the log K_{aw} using both QSAR (EPI Suite HENRYWIN) and DFT methods. To our knowledge, there are currently no experimental results available for the PPDQs. Therefore, seven test compounds with experimental results reported in Abraham *et al.* (2019) were used to test these predictive models.[64] These test compounds were selected for their structural similarities to

PPDQs and have experimental log K_{aw} results between -8.57 and -2.42 (Table S4). Figure S7 plots predicted versus experimental log K_{aw} values using both DFT and EPI Suite methods. The results indicate better agreement between experimental values and predicted values obtained with DFT calculations (slope = 1.04, R^2 = 0.89) versus EPI Suite (slope = 0.73, R^2 = 0.65). As seen in Table 2, the HENRYWIN predictions underestimate K_{aw} by 2–4 orders of magnitude relative to DFT for the PPDQs, consistent with the variance observed in the water solubility values. Furthermore, the DFT predictions for 6PPDQ agree with COSMOtherm predictions, which calculated the log K_{aw} to be -8.28.[65] The increased performance of DFT relative to EPI Suite in this case may be due to the accuracy of DFT at describing molecules in the gas phase, combined with the lack of similarity of the PPDQs to the molecules in the training sets used by QSAR methods like HENRYWIN. Therefore, we recommend the use DFT rather than QSAR methods for the prediction of log K_{aw}.

The DFT calculated log K_{aw} values for the PPDQs reported in Table 2 range from -7.2 for 77PDQ to -8.9 for DTPDQ with 6PPDQ predicted to be -8.0. For context, these values are considerably lower than pollutants observed to exhibit long range atmospheric transport, such as polychlorinated biphenyls (-2 to -3), and are in a similar range to atrazine (-6.9) and carbaryl (-7.7)[17] which are not. As such, PPDQs are not expected to readily partition from water into the gas phase. It remains unclear what process is responsible for the decrease in aqueous concentrations of PPDQs in open containers. To date we have not observed any direct evidence of gas phase PPDQ arising from aqueous solution. While this observation is consistent with the low predicted K_{aw} values predicted here, experimentally determined K_{aw} are a recognized knowledge gap that may further elucidate the underlying loss mechanism.

Conclusions

Physicochemical properties may be measured through experimentation and predicted with computational approaches including QSARs and DFT methods. Here, we report experimental water solubilities for 6PPDQ (31 ± 5 μg L^{-1}) and five structural analogs, ranging from 3.5 ± 0.3 μg L^{-1} for DTPDQ

to 168 ± 8 μg L^{-1} for DPPDQ. EPI Suite predictions based QSARs methods were 2–5 orders of magnitude greater than experimental solubility results, potentially due to the anomalously low basicity of the PPDQ amines which is not represented in the QSAR training set. Re-parameterization of the equation used by WSKOWWIN significantly improved these predictions. Examining log K_{ow}, we found that EPI Suite predicted values in close agreement with experimental findings. The KOWWIN predicted log K_{ow} values ranged from 2.58 for IPPDQ to 5.47 for 77PPDQ, suggesting that they pose a bioaccumulation risk if persistent. While DFT predicted a similar trend and rank order among the PPDQs investigated here, it systematically underestimated log K_{ow}, which may be due to the lack of specific solvent-solute interactions in the DFT model applied. Conversely, we found DFT worked well in predicting air-water partitioning for a series of test compounds, but as we were unable to detect gas phase concentrations we do not report experimental K_{aw} values for PPDQs. DFT predicted low log K_{aw} values for PPDQs, ranging from -7.2 for 77PDQ to -8.9 for DTPDQ, suggesting that atmospheric transport in the gas phase is unlikely. This work presents both experimental and computed physicochemical properties for these emerging contaminants. As computational approaches become increasingly powerful and accessible, we encourage users to critically evaluate their fitness for specific purposes. An abundance of computational results with unknown accuracy may prove more hindrance than help if applied inappropriately or used in place of experimental data.

Author Contributions

Simon H. Maguire – conceptualization, formal analysis, investigation, methodology, software, validation, visualization, writing – original draft, writing – review & editing.

Misha Zvekic – conceptualization, formal analysis, investigation, methodology, validation, visualization, writing – original draft, writing – review & editing.

Angelina Jaeger – investigation, methodology, validation, writing – original draft, writing – review & editing.

Joseph Monaghan – formal analysis, methodology, software, writing – review & editing.

Erik T. Krogh – conceptualization, funding acquisition, methodology, project administration, resources, supervision, writing – original draft, writing – review & editing.

Heather A. Wiebe – conceptualization, funding acquisition, methodology, project administration, resources, supervision, writing – original draft, writing – review & editing.

Conflicts of interest

There are no conflicts to declare.

Acknowledgements

The authors acknowledge the ongoing support of students and infrastructure from Vancouver Island University and the University of Victoria. This work was supported by funding provided by NSERC Discovery (ETK RGPIN-2022-05349; HW RGPIN-2021-02916), Mitacs Accelerate (IT27105), and BC Salmon Restoration and Innovation Fund (BCSRIF_2022_389). This work was enabled in part by the support provided by the Canadian Foundation for Innovation (32238), the BC DRI Group, and the Digital Research Alliance of Canada (alliancecan.ca).

Notes and references

(1) Tian, Z.; Zhao, H.; Peter, K. T.; Gonzalez, M.; Wetzel, J.; Wu, C.; Hu, X.; Prat, J.; Mudrock, E.; Hettinger, R.; Cortina, A. E.; Biswas, R. G.; Kock, F. V. C.; Soong, R.; Jenne, A.; Du, B.; Hou, F.; He, H.; Lundeen, R.; Gilbreath, A.; Sutton, R.; Scholz, N. L.; Davis, J. W.; Dodd, M. C.; Simpson, A.; McIntyre, J. K.; Kolodziej, E. P. A Ubiquitous Tire Rubber–Derived Chemical Induces Acute Mortality in Coho Salmon. *Science* **2021**, *371* (6525), 185–189. https://doi.org/10.1126/science.abd6951.

(2) Hiki, K.; Yamamoto, H. Concentration and Leachability of *N*-(1,3-Dimethylbutyl)-*N*′-Phenyl-*p*-Phenylenediamine (6PPD) and Its Quinone Transformation Product (6PPD-Q) in Road Dust Collected in Tokyo, Japan. *Environmental Pollution* **2022**, *302*, 119082. https://doi.org/10.1016/j.envpol.2022.119082.

(3) Zhu, J.; Guo, R.; Ren, F.; Jiang, S.; Jin, H. Occurrence and Partitioning of *p*-Phenylenediamine Antioxidants and Their Quinone Derivatives in Water and Sediment. *Science of The Total Environment* **2024**, *914*, 170046. https://doi.org/10.1016/j.scitotenv.2024.170046.

(4) Monaghan, J.; Jaeger, A.; Jai, J. K.; Tomlin, H.; Atkinson, J.; Brown, T. M.; Gill, C. G.; Krogh, E. T. Automated, High-Throughput Analysis of Tire-Derived p-Phenylenediamine Quinones (PPDQs) in Water by Online Membrane Sampling Coupled to MS/MS. *ACS EST Water* **2023**, *3* (10), 3293–3304. https://doi.org/10.1021/acsestwater.3c00275.

(5) Nair, P.; Sun, J.; Xie, L.; Kennedy, L.; Kozakiewicz, D.; Kleywegt, S.; Hao, C.; Byun, H.; Barrett, H.; Baker, J.; Monaghan, J.; Krogh, E.; Song, D.; Peng, H. Synthesis and Toxicity Evaluation of Tire Rubber-Derived Quinones. ChemRxiv June 19, 2023. https://doi.org/10.26434/chemrxiv-2023-pmxvc.

(6) Zhao, H. N.; Hu, X.; Gonzalez, M.; Rideout, C. A.; Hobby, G. C.; Fisher, M. F.; McCormick, C. J.; Dodd, M. C.; Kim, K. E.; Tian, Z.; Kolodziej, E. P. Screening P-Phenylenediamine Antioxidants, Their Transformation Products, and Industrial Chemical Additives in Crumb Rubber and Elastomeric Consumer Products. *Environ. Sci. Technol.* **2023**, *57* (7), 2779–2791. https://doi.org/10.1021/acs.est.2c07014.

(7) Zhang, Z.; Dai, C.; Chen, S.; Hu, H.; Kang, R.; Xu, X.; Huo, X. Spatiotemporal Variation of 6PPD and 6PPDQ in Dust and Soil from E-Waste Recycling Areas. *Science of The Total Environment* **2024**, *923*, 171495. https://doi.org/10.1016/j.scitotenv.2024.171495.
(8) Olubusoye, B. S.; Cizdziel, J. V.; Bee, M.; Moore, M. T.; Pineda, M.; Yargeau, V.; Bennett, E. R. Toxic Tire Wear Compounds (6PPD-Q and 4-ADPA) Detected in Airborne Particulate Matter Along a Highway in Mississippi, USA. *Bull Environ Contam Toxicol* **2023**, *111* (6), 68. https://doi.org/10.1007/s00128-023-03820-7.
(9) Brinkmann, M.; Montgomery, D.; Selinger, S.; Miller, J. G. P.; Stock, E.; Alcaraz, A. J.; Challis, J. K.; Weber, L.; Janz, D.; Hecker, M.; Wiseman, S. Acute Toxicity of the Tire Rubber-Derived Chemical 6PPD-Quinone to Four Fishes of Commercial, Cultural, and Ecological Importance. *Environ. Sci. Technol. Lett.* **2022**, *9* (4), 333–338. https://doi.org/10.1021/acs.estlett.2c00050.
(10) Montgomery, D.; Ji, X.; Cantin, J.; Philibert, D.; Foster, G.; Selinger, S.; Jain, N.; Miller, J.; McIntyre, J.; de Jourdan, B.; Wiseman, S.; Hecker, M.; Brinkmann, M. Interspecies Differences in 6PPD-Quinone Toxicity Across Seven Fish Species: Metabolite Identification and Semiquantification. *Environ. Sci. Technol.* **2023**, *57* (50), 21071–21079. https://doi.org/10.1021/acs.est.3c06891.
(11) Philibert, D.; Stanton, R. S.; Tang, C.; Stock, N. L.; Benfey, T.; Pirrung, M.; de Jourdan, B. The Lethal and Sublethal Impacts of Two Tire Rubber-Derived Chemicals on Brook Trout (Salvelinus Fontinalis) Fry and Fingerlings. *Chemosphere* **2024**, *360*, 142319. https://doi.org/10.1016/j.chemosphere.2024.142319.
(12) Roberts, C.; Lin, J.; Kohlman, E.; Jain, N.; Amekor, M.; Alcaraz, A. J.; Hogan, N.; Hecker, M.; Brinkmann, M. Acute and Subchronic Toxicity of 6PPD-Quinone to Early Life Stage Lake Trout (Salvelinus Namaycush). *Environ. Sci. Technol.* **2025**. https://doi.org/10.1021/acs.est.4c09090.
(13) Tian, Z.; Gonzalez, M.; Rideout, C. A.; Zhao, H. N.; Hu, X.; Wetzel, J.; Mudrock, E.; James, C. A.; McIntyre, J. K.; Kolodziej, E. P. 6PPD-Quinone: Revised Toxicity Assessment and Quantification with a Commercial Standard. *Environ. Sci. Technol. Lett.* **2022**, *9* (2), 140–146. https://doi.org/10.1021/acs.estlett.1c00910.
(14) Lo, B. P.; Marlatt, V. L.; Liao, X.; Reger, S.; Gallilee, C.; Ross, A. R. S.; Brown, T. M. Acute Toxicity of 6PPD-Quinone to Early Life Stage Juvenile Chinook (Oncorhynchus Tshawytscha) and Coho (Oncorhynchus Kisutch) Salmon. *Environ Toxicol Chem* **2023**, *42* (4), 815–822. https://doi.org/10.1002/etc.5568.
(15) Di, S.; Liu, Z.; Zhao, H.; Li, Y.; Qi, P.; Wang, Z.; Xu, H.; Jin, Y.; Wang, X. Chiral Perspective Evaluations: Enantioselective Hydrolysis of 6PPD and 6PPD-Quinone in Water and Enantioselective Toxicity to *Gobiocypris Rarus* and *Oncorhynchus Mykiss*. *Environment International* **2022**, *166*, 107374. https://doi.org/10.1016/j.envint.2022.107374.
(16) United States Tire Manufacturer's Association. *Preliminary (Stage 1) Alternatives Analysis Report*; 2024. https://www.ustires.org/system/files/files/2024-08/USTMA%206PPD%20Consortium%20Revised%20Preliminary%20AA%20Report_July_2024.pdf.
(17) Schwarzenbach, R. P.; Gschwend, P. M.; Imboden, D. M. *Environmental Organic Chemistry*, 3rd edition.; Wiley: Hoboken, N.J, 2016.
(18) Schwarzenbach, R. P.; Escher, B. I.; Fenner, K.; Hofstetter, T. B.; Johnson, C. A.; von Gunten, U.; Wehrli, B. The Challenge of Micropollutants in Aquatic Systems. *Science* **2006**, *313* (5790), 1072–1077. https://doi.org/10.1126/science.1127291.
(19) Hu, X.; Zhao, H. (Nina); Tian, Z.; Peter, K. T.; Dodd, M. C.; Kolodziej, E. P. Chemical Characteristics, Leaching, and Stability of the Ubiquitous Tire Rubber-Derived Toxicant 6PPD-Quinone. *Environ. Sci.: Processes Impacts* **2023**, *25* (5), 901–911. https://doi.org/10.1039/D3EM00047H.
(20) Lane, R. F.; Smalling, K. L.; Bradley, P. M.; Greer, J. B.; Gordon, S. E.; Hansen, J. D.; Kolpin, D. W.; Spanjer, A. R.; Masoner, J. R. Tire-Derived Contaminants 6PPD and 6PPD-Q: Analysis, Sample

Handling, and Reconnaissance of United States Stream Exposures. *Chemosphere* **2024**, *363*, 142830. https://doi.org/10.1016/j.chemosphere.2024.142830.
(21) Borden, S. A.; Damer, H. N.; Krogh, E. T.; Gill, C. G. Direct Quantitation and Characterization of Fatty Acids in Salmon Tissue by Condensed Phase Membrane Introduction Mass Spectrometry (CP-MIMS) Using a Modified Donor Phase. *Anal Bioanal Chem* **2019**, *411* (2), 291–303. https://doi.org/10.1007/s00216-018-1467-y.
(22) Nuñez, J. R.; Colby, S. M.; Thomas, D. G.; Tfaily, M. M.; Tolic, N.; Ulrich, E. M.; Sobus, J. R.; Metz, T. O.; Teeguarden, J. G.; Renslow, R. S. Evaluation of In Silico Multifeature Libraries for Providing Evidence for the Presence of Small Molecules in Synthetic Blinded Samples. *J. Chem. Inf. Model.* **2019**, *59* (9), 4052–4060. https://doi.org/10.1021/acs.jcim.9b00444.
(23) US EPA, O. *EPI Suite™-Estimation Program Interface*. https://www.epa.gov/tsca-screening-tools/epi-suitetm-estimation-program-interface (accessed 2024-07-30).
(24) Wittekindt, C.; Goss, K.-U. Screening the Partition Behavior of a Large Number of Chemicals with a Quantum-Chemical Software. *Chemosphere* **2009**, *76* (4), 460–464. https://doi.org/10.1016/j.chemosphere.2009.03.046.
(25) Harris, D. C. *Quantitative Chemical Analysis*; W H Freeman & Co: New York, 2015.
(26) Klöckner, P.; Seiwert, B.; Wagner, S.; Reemtsma, T. Organic Markers of Tire and Road Wear Particles in Sediments and Soils: Transformation Products of Major Antiozonants as Promising Candidates. *Environ. Sci. Technol.* **2021**, *55* (17), 11723–11732. https://doi.org/10.1021/acs.est.1c02723.
(27) Cao, G.; Wang, W.; Zhang, J.; Wu, P.; Zhao, X.; Yang, Z.; Hu, D.; Cai, Z. New Evidence of Rubber-Derived Quinones in Water, Air, and Soil. *Environ. Sci. Technol.* **2022**, *56* (7), 4142–4150. https://doi.org/10.1021/acs.est.1c07376.
(28) Zeng, L.; Li, Y.; Sun, Y.; Liu, L.-Y.; Shen, M.; Du, B. Widespread Occurrence and Transport of P-Phenylenediamines and Their Quinones in Sediments across Urban Rivers, Estuaries, Coasts, and Deep-Sea Regions. *Environ. Sci. Technol.* **2023**, *57* (6), 2393–2403. https://doi.org/10.1021/acs.est.2c07652.
(29) Leach, A. R. *Molecular Modelling: Principles and Applications*; Prentice Hall, 2001.
(30) Cramer, C. J. *Essentials of Computational Chemistry: Theories and Models*; Wiley, 2005.
(31) van Mourik, T.; Bühl, M.; Gaigeot, M.-P. Density Functional Theory across Chemistry, Physics and Biology. *Philos Trans A Math Phys Eng Sci* **2014**, *372* (2011), 20120488. https://doi.org/10.1098/rsta.2012.0488.
(32) Miertuš, S.; Scrocco, E.; Tomasi, J. Electrostatic Interaction of a Solute with a Continuum. A Direct Utilizaion of AB Initio Molecular Potentials for the Prevision of Solvent Effects. *Chemical Physics* **1981**, *55* (1), 117–129. https://doi.org/10.1016/0301-0104(81)85090-2.
(33) Marenich, A. V.; Cramer, C. J.; Truhlar, D. G. Universal Solvation Model Based on Solute Electron Density and on a Continuum Model of the Solvent Defined by the Bulk Dielectric Constant and Atomic Surface Tensions. *J. Phys. Chem. B* **2009**, *113* (18), 6378–6396. https://doi.org/10.1021/jp810292n.
(34) Vandergrift, G. W.; Lattanzio-Battle, W.; Krogh, E. T.; Gill, C. G. Condensed Phase Membrane Introduction Mass Spectrometry with In Situ Liquid Reagent Chemical Ionization in a Liquid Electron Ionization Source (CP-MIMS-LEI/CI). *J. Am. Soc. Mass Spectrom.* **2020**, *31* (4), 908–916. https://doi.org/10.1021/jasms.9b00143.
(35) Frisch, M. J.; Trucks, G. W.; Schlegel, H. B.; Scuseria, G. E.; Robb, M. A.; Cheeseman, J. R.; Scalmani, G.; Barone, V.; Petersson, G. A.; Nakatsuji, H.; Li, X.; Caricato, M.; Marenich, A. V.; Bloino, J.; Janesko, B. G.; Gomperts, R.; Mennucci, B.; Hratchian, H. P.; Ortiz, J. V.; Izmaylov, A. F.; Sonnenberg, J. L.; Williams; Ding, F.; Lipparini, F.; Egidi, F.; Goings, J.; Peng, B.; Petrone, A.; Henderson, T.; Ranasinghe, D.; Zakrzewski, V. G.; Gao, J.; Rega, N.; Zheng, G.; Liang, W.; Hada, M.;

Ehara, M.; Toyota, K.; Fukuda, R.; Hasegawa, J.; Ishida, M.; Nakajima, T.; Honda, Y.; Kitao, O.; Nakai, H.; Vreven, T.; Throssell, K.; Montgomery Jr., J. A.; Peralta, J. E.; Ogliaro, F.; Bearpark, M. J.; Heyd, J. J.; Brothers, E. N.; Kudin, K. N.; Staroverov, V. N.; Keith, T. A.; Kobayashi, R.; Normand, J.; Raghavachari, K.; Rendell, A. P.; Burant, J. C.; Iyengar, S. S.; Tomasi, J.; Cossi, M.; Millam, J. M.; Klene, M.; Adamo, C.; Cammi, R.; Ochterski, J. W.; Martin, R. L.; Morokuma, K.; Farkas, O.; Foresman, J. B.; Fox, D. J. Gaussian 16 Rev. C.01, 2016.

(36) Bussi, G.; Donadio, D.; Parrinello, M. Canonical Sampling through Velocity Rescaling. *J Chem Phys* **2007**, *126* (1), 014101. https://doi.org/10.1063/1.2408420.

(37) M, B.; G, B. Pressure Control Using Stochastic Cell Rescaling. *The Journal of chemical physics* **2020**, *153* (11). https://doi.org/10.1063/5.0020514.

(38) Termopoli, V.; Famiglini, G.; Palma, P.; Cappiello, A.; Vandergrift, G. W.; Krogh, E. T.; Gill, C. G. Condensed Phase Membrane Introduction Mass Spectrometry with Direct Electron Ionization: On-Line Measurement of PAHs in Complex Aqueous Samples. *J. Am. Soc. Mass Spectrom.* **2016**, *27* (2), 301–308. https://doi.org/10.1007/s13361-015-1285-9.

(39) Hiki, K.; Asahina, K.; Kato, K.; Yamagishi, T.; Omagari, R.; Iwasaki, Y.; Watanabe, H.; Yamamoto, H. Acute Toxicity of a Tire Rubber-Derived Chemical, 6PPD Quinone, to Freshwater Fish and Crustacean Species. *Environ. Sci. Technol. Lett.* **2021**, *8* (9), 779–784. https://doi.org/10.1021/acs.estlett.1c00453.

(40) Hess, B. Determining the Shear Viscosity of Model Liquids from Molecular Dynamics Simulations. *The Journal of Chemical Physics* **2002**, *116* (1), 209–217. https://doi.org/10.1063/1.1421362.

(41) Wiebe, H.; Spooner, J.; Boon, N.; Deglint, E.; Edwards, E.; Dance, P.; Weinberg, N. Calculation of Molecular Volumes and Volumes of Activation Using Molecular Dynamics Simulations. *J. Phys. Chem. C* **2012**, *116* (3), 2240–2245. https://doi.org/10.1021/jp209088u.

(42) Spooner, J.; Wiebe, H.; Boon, N.; Deglint, E.; Edwards, E.; Yanciw, B.; Patton, B.; Thiele, L.; Dance, P.; Weinberg, N. Molecular Dynamics Calculation of Molecular Volumes and Volumes of Activation. *Phys. Chem. Chem. Phys.* **2012**, *14* (7), 2264–2277. https://doi.org/10.1039/C2CP22949H.

(43) Abraham, M. J.; Murtola, T.; Schulz, R.; Páll, S.; Smith, J. C.; Hess, B.; Lindahl, E. GROMACS: High Performance Molecular Simulations through Multi-Level Parallelism from Laptops to Supercomputers. *SoftwareX* **2015**, *1–2*, 19–25. https://doi.org/10.1016/j.softx.2015.06.001.

(44) Jorgensen, W. L.; Maxwell, D. S.; Tirado-Rives, J. Development and Testing of the OPLS All-Atom Force Field on Conformational Energetics and Properties of Organic Liquids. *J. Am. Chem. Soc.* **1996**, *118* (45), 11225–11236. https://doi.org/10.1021/ja9621760.

(45) Monaghan, J.; Jaeger, A.; Agua, A. R.; Stanton, R. S.; Pirrung, M.; Gill, C. G.; Krogh, E. T. A Direct Mass Spectrometry Method for the Rapid Analysis of Ubiquitous Tire-Derived Toxin N-(1,3-Dimethylbutyl)-N'-Phenyl-p-Phenylenediamine Quinone (6-PPDQ). *Environ. Sci. Technol. Lett.* **2021**, *8* (12), 1051–1056. https://doi.org/10.1021/acs.estlett.1c00794.

(46) Tuttle, M. R.; Davis, S. T.; Zhang, S. Synergistic Effect of Hydrogen Bonding and π–π Stacking Enables Long Cycle Life in Organic Electrode Materials. *ACS Energy Lett.* **2021**, *6* (2), 643–649. https://doi.org/10.1021/acsenergylett.0c02604.

(47) Klöckner, P.; Seiwert, B.; Eisentraut, P.; Braun, U.; Reemtsma, T.; Wagner, S. Characterization of Tire and Road Wear Particles from Road Runoff Indicates Highly Dynamic Particle Properties. *Water Research* **2020**, *185*, 116262. https://doi.org/10.1016/j.watres.2020.116262.

(48) Greer, J. B.; Dalsky, E. M.; Lane, R. F.; Hansen, J. D. Establishing an In Vitro Model to Assess the Toxicity of 6PPD-Quinone and Other Tire Wear Transformation Products. *Environ. Sci. Technol. Lett.* **2023**, *10* (6), 533–537. https://doi.org/10.1021/acs.estlett.3c00196.

(49) Tebes-Stevens*, C.; Patel, J. M.; Koopmans, M.; Olmstead, J.; Hilal, S. H.; Pope, N.; Weber, E. J.; Wolfe, K. Demonstration of a Consensus Approach for the Calculation of Physicochemical

Properties Required for Environmental Fate Assessments. *Chemosphere* **2018**, *194*, 94–106. https://doi.org/10.1016/j.chemosphere.2017.11.137.
(50) Vilas-Boas, S. M.; da Costa, M. C.; Coutinho, J. A. P.; Ferreira, O.; Pinho, S. P. Octanol–Water Partition Coefficients and Aqueous Solubility Data of Monoterpenoids: Experimental, Modeling, and Environmental Distribution. *Ind. Eng. Chem. Res.* **2022**, *61* (8), 3154–3167. https://doi.org/10.1021/acs.iecr.1c04196.
(51) Endo, S.; Hammer, J.; Matsuzawa, S. Experimental Determination of Air/Water Partition Coefficients for 21 Per- and Polyfluoroalkyl Substances Reveals Variable Performance of Property Prediction Models. *Environ. Sci. Technol.* **2023**, *57* (22), 8406–8413. https://doi.org/10.1021/acs.est.3c02545.
(52) Schönsee, C. D.; Bucheli, T. D. Experimental Determination of Octanol–Water Partition Coefficients of Selected Natural Toxins. *J. Chem. Eng. Data* **2020**, *65* (4), 1946–1953. https://doi.org/10.1021/acs.jced.9b01129.
(53) Rodríguez-Leal, I.; MacLeod, M. The Applicability Domain of EPI Suite™ for Screening Phytotoxins for Potential to Contaminate Source Water for Drinking. *Environmental Sciences Europe* **2022**, *34* (1), 96. https://doi.org/10.1186/s12302-022-00676-2.
(54) Boethling, R.; Meylan, W. How Accurate Are Physical Property Estimation Programs for Organosilicon Compounds? *Environmental Toxicology and Chemistry* **2013**, *32* (11), 2433–2440. https://doi.org/10.1002/etc.2326.
(55) Van Der Spoel, D.; Manzetti, S.; Zhang, H.; Klamt, A. Prediction of Partition Coefficients of Environmental Toxins Using Computational Chemistry Methods. *ACS Omega* **2019**, *4* (9), 13772–13781. https://doi.org/10.1021/acsomega.9b01277.
(56) Llompart, P.; Minoletti, C.; Baybekov, S.; Horvath, D.; Marcou, G.; Varnek, A. Will We Ever Be Able to Accurately Predict Solubility? *Sci Data* **2024**, *11* (1), 303. https://doi.org/10.1038/s41597-024-03105-6.
(57) Veith, G. D.; Austin, N. M.; Morris, R. T. A Rapid Method for Estimating Log P for Organic Chemicals. *Water Research* **1979**, *13* (1), 43–47. https://doi.org/10.1016/0043-1354(79)90252-5.
(58) Namjesnik-Dejanovic, K.; Cabaniss, S. E. Reverse-Phase HPLC Method for Measuring Polarity Distributions of Natural Organic Matter. *Environ. Sci. Technol.* **2004**, *38* (4), 1108–1114. https://doi.org/10.1021/es0344157.
(59) Hodges, G.; Eadsforth, C.; Bossuyt, B.; Bouvy, A.; Enrici, M.-H.; Geurts, M.; Kotthoff, M.; Michie, E.; Miller, D.; Müller, J.; Oetter, G.; Roberts, J.; Schowanek, D.; Sun, P.; Venzmer, J. A Comparison of Log Kow (n-Octanol–Water Partition Coefficient) Values for Non-Ionic, Anionic, Cationic and Amphoteric Surfactants Determined Using Predictions and Experimental Methods. *Environmental Sciences Europe* **2019**, *31* (1), 1. https://doi.org/10.1186/s12302-018-0176-7.
(60) Sühring, R.; Mayer, P.; Leonards, P.; MacLeod, M. Fate-Directed Risk Assessment of Chemical Mixtures: A Case Study for Cedarwood Essential Oil. *Environ. Sci.: Processes Impacts* **2022**, *24* (8), 1133–1143. https://doi.org/10.1039/D2EM00103A.
(61) Cappelli, C. I.; Benfenati, E.; Cester, J. Evaluation of QSAR Models for Predicting the Partition Coefficient (Log *P*) of Chemicals under the REACH Regulation. *Environmental Research* **2015**, *143*, 26–32. https://doi.org/10.1016/j.envres.2015.09.025.
(62) Chi, Y.; Zhang, H.; Huang, Q.; Lin, Y.; Ye, G.; Zhu, H.; Dong, S. Environmental Risk Assessment of Selected Organic Chemicals Based on TOC Test and QSAR Estimation Models. *Journal of Environmental Sciences* **2018**, *64*, 23–31. https://doi.org/10.1016/j.jes.2016.11.018.
(63) Jones, M. R.; Brooks, B. R. Quantum Chemical Predictions of Water–Octanol Partition Coefficients Applied to the SAMPL6 logP Blind Challenge. *J Comput Aided Mol Des* **2020**, *34* (5), 485–493. https://doi.org/10.1007/s10822-020-00286-1.

(64) Abraham, M. H.; Acree, W. E.; Hoekman, D.; Leo, A. J.; Medlin, M. L. A New Method for the Determination of Henry's Law Constants (Air-Water-Partition Coefficients). *Fluid Phase Equilibria* **2019**, *502*, 112300. https://doi.org/10.1016/j.fluid.2019.112300.
(65) Rodgers, T. F. M.; Wang, Y.; Humes, C.; Jeronimo, M.; Johannessen, C.; Spraakman, S.; Giang, A.; Scholes, R. C. Bioretention Cells Provide a 10-Fold Reduction in 6PPD-Quinone Mass Loadings to Receiving Waters: Evidence from a Field Experiment and Modeling. *Environ. Sci. Technol. Lett.* **2023**, *10* (7), 582–588. https://doi.org/10.1021/acs.estlett.3c00203.